

# Improving and characterizing the burst-hardware injection pipeline for GEO600

Luis M. Colón Pérez  
Department of Physics, University of Puerto Rico, San Juan PR 00931  
colonperez@gmail.com

---

## Abstract

In this work we present hardware injections made into the GEO600 in order to verify the performance of its trigger algorithm mHACR. We present an improved hardware/software injection pipeline for the gravitational-wave detector GEO 600. The pipeline was designed such that it allows injections of a wide variety of burst gravitational waveforms. We demonstrate the injection pipeline by performing hardware injections in GEO 600, and present a preliminary analysis on the hardware injections using the mHACR burst detection algorithm.

---

## 1. Introduction

A network of gravitational wave (GW) detectors is currently operating or being commissioned around the world. Some of these are: AIGO, in Australia, TAMA, in Japan, VIRGO, in Italy, and LIGO, in the United States. Also there is GEO600<sup>[1]</sup> which is a German/British GW detector near Hannover, Germany.

One of the main searches in these GW detectors is for transient, unmodelled GW bursts<sup>[2]</sup>. The nature of those signals is in such a way that it will be difficult to distinguish it from an instrumental or external burst which can couple into the main detector output, meanwhile some channels might be sensitive enough that a GW might couple in these channels. Therefore great effort is made in order to understand the system and to develop instrumental veto techniques to cut down the event rate.

The detection algorithms used to search for signatures of GW bursts in the data of these detectors typically use time-frequency detection methods. The burst detection algorithm employed in the data characterization of GEO 600 is called mHACR. It is important to characterize the detection algorithms by studying their efficiency of detecting burst waveforms in the data with a given 'false alarm' rate. This is traditionally done by 'injecting' known waveforms into the detector, or, into the data and by performing the analysis using the detection algorithms. Previous performance tests were done on mHACR and HACR\*, employing only sine-Gaussians waveforms<sup>[2,4,5,6]</sup>. These were of particular preference because of their well defined parameters, like central frequency, total power etc. In order to properly characterize the performance of the detection algorithm (like its detection efficiency, false alarm rate, accuracy of the parameter estimation etc) it is necessary to repeat these performance tests on a wide morphology of burst waveforms. The forms can be unphysical waves containing more uncertainty than

---

\* The previous detection algorithm used in GEO600.

the sine-Gaussians in their description and different physical waveforms like the ones predicted to appear as strains in the detectors main output channel. These waveforms can be burst waveforms expected from astrophysical sources like core-collapse supernovae, black hole ring downs etc., or some 'ad-hoc' waveforms like Gaussian-modulated sinusoidal waveforms.

In this report, we present an improved burst hardware/software injection pipeline for GEO 600 detector. The pipeline is designed in such a way that a number of (randomly chosen) burst waveforms can be injected into the detector or to the data. The parameters of the injected waveforms are chosen from a large parameter range. We also do a preliminary characterization of the injection pipeline and mHACR detection algorithm by performing hardware injections into GEO 600 and subsequently analyzing the data.

In Sec. 2, we describe the HW/SW injection pipeline. Sec. 3 provides an overview of burst waveforms used for the injections. Sec. 5 provides a brief description of the mHACR detection algorithm. In Sec. 6, we discuss the injections performed in GEO 600, and, in Sec. 7, we conclude.

## 2. A burst HW/SW injection pipeline for GEO600

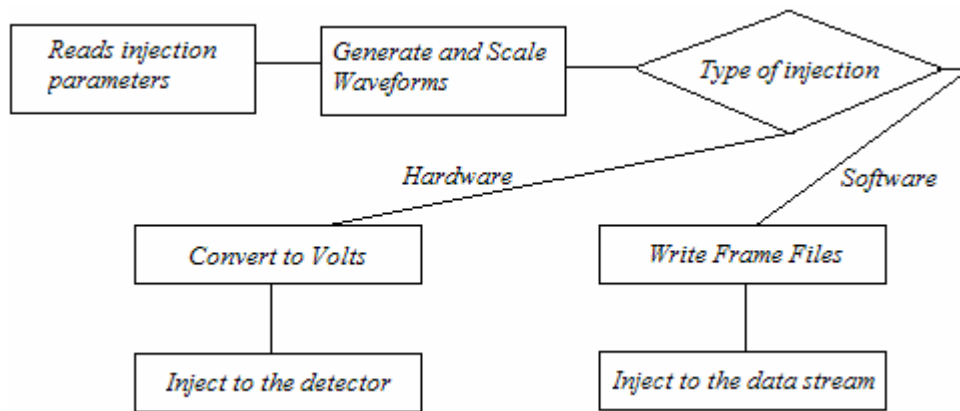


Figure 1. A block diagram of the injection pipeline script.

A block diagram of the injection pipeline is given in Fig. 1. The first step of the pipeline is to read the injection parameter file, which contains the range of the parameters for each of the injected waveforms. After the ranges of the parameters are set “Generate and Scale Waveforms” block, randomly chooses one of the desired waveforms and randomly chooses the parameters of the particular waveform chosen, from the ranges set by the user in the injection parameter file. Then it generates the waveform from these randomly created parameters.

In the case of HW injections, after generating the waveform this signal must be converted to voltage as fig. 1 shows, so that, when applied differentially Michelson length-control actuators, it gives the differential displacement expected from the waveform desired to inject. The signal is then sent to the signal injection hardware and finally is applied to the length control actuators of the Michelson control servo to create the desired differential

arm-length changes<sup>[6]</sup>. In the case of SW injections the signals are then applied to the data stream output of the  $h(t)$  channel.

### 3. Burst waveforms

The script, either for HW or SW, randomly injects unphysical and physical waveforms. For unphysical or ad-hoc waveforms we mean, Gaussians, sine-Gaussians and Gaussians noise bursts. For physical waveforms we mean, blackhole ringdowns and supernova core collapses. In this section, we summarize the burst waveforms used for the injections.

#### 3.1 Gaussian waveforms

$$h(t) = h_{r_{SS}} \left( \frac{2}{\tau^2 \pi} \right)^{1/4} e^{\left( \frac{-(t-t_0)^2}{\tau^2} \right)} \quad (1)$$

The Gaussian waveforms in the time domain are given by eq. 1, where  $t_0$ , stands for the center time of the waveform,  $\tau$ , is the width of the Gaussian wave packet, and  $h_{r_{SS}}$ , a characteristic amplitude such that the power in the wave form is  $h_{r_{SS}}^2$ .

#### 3.2 Sine-Gaussian waveforms

$$h(t) = h_{r_{SS}} \left( \frac{2f_0^2}{\pi} \right)^{1/4} \sin(2\pi f_0(t-t_0)) e^{\left( \frac{-(t-t_0)^2}{2\tau^2} \right)} \quad (2)$$

The sine Gaussian waveform in the time domain is given by eq. 2, where  $f_0$ , stands for the central frequency of the wave,  $\tau$ , is the width of the Gaussian which is related to the quality factor,  $Q$ , by  $\tau = Q/(\sqrt{2\pi}f_0)$ , as the Gaussian  $t_0$ , stands for the central time of the waveform, and  $h_{r_{SS}}$ , the scaling amplitude such that the power in the waveform is  $h_{r_{SS}}^2$ .

#### 3.3 Gaussian-modulated noise bursts

$$h(t) = h_{r_{SS}} \left( \frac{2}{\tau^2 \pi} \right)^{1/4} n(t) e^{\left( \frac{-(t-t_0)^2}{\tau^2} \right)} \quad (3)$$

These waveforms are produced by modulating white noise with a Gaussian function in time domain. In the above equation  $t_0$ , stands for the central time of the waveform,  $\tau$ , is the width of the Gaussian wave,  $h_{r_{SS}}$ , the scaling amplitude, and  $n(t)$  stands for white noise. The  $n(t)$  is a vector of pseudorandom values drawn from a normal distribution with mean zero and standard deviation of 1. For these waveforms, the total power contained will not be exactly equal to  $h_{r_{SS}}^2$ , since it deviates by a factor that changes in time because of the noise presence.

#### 3.4 Black hole ringdown waveforms

For the ringdown we consider only the radiation emitted in the dominant mode of:  $l=m=2$ <sup>[7]</sup>. Therefore the waveform is given by a decaying sinusoid. The quasi-normal mode frequency of the black hole is given by,

$$f_{QNR} = [1 - 0.63(1 - a)^{\frac{3}{10}}] \frac{1}{2\pi M} \quad (4)$$

Where  $a$ , is the Kerr parameter, which is allowed to vary between 0 (non-spinning case) and 0.98 (maximally spinning case), and  $M$ , the total mass of the black hole. The quality factor,  $Q_{RD}$ , of the waveform is given by,

$$Q_{RD} = 2(1 - a)^{-\frac{9}{20}} \quad (5)$$

and,

$$A = \sqrt{\frac{128\eta^2 \varepsilon}{M f_{QNR} Q_{RD}}} \quad (6)$$

is a dimensionless coefficient describing the magnitude of the perturbation when the ringdown begins.  $\eta = \mu / M$ , where  $\mu$  is the reduced mass of the binary, and  $\varepsilon$ , is the fraction of mass converted into gravitational waves during ringdown. The amplitude of the waveform measured at the detector would be,

$$A_{RD} = \frac{AM}{d_{ringdown}} \sqrt{F_+^2 + F_\times^2} \left| {}_2S_2^2 \right| \quad (7)$$

$\left| {}_2S_2^2 \right|$ , is the spin weighted spheroidal harmonic that depends on the inclination angle of the black hole spin axis seen from the observer and the Kerr parameter, and  $d_{ringdown}$ , is the distance from the ringdown source to the detector.  $F_+$  and  $F_\times$  are the antenna pattern functions for the two polarizations, given by,

$$F_+ = \frac{1}{2}(1 + \cos^2 \theta) \cos 2\varphi \cos 2\psi - \cos \theta \sin 2\varphi \sin 2\psi \quad (8)$$

$$F_\times = \frac{1}{2}(1 + \cos^2 \theta) \cos 2\varphi \sin 2\psi + \cos \theta \sin 2\varphi \cos 2\psi \quad (9)$$

The angles  $(\theta, \varphi)$  determine the direction of the source in the sky in the detector frame and  $\psi$ , is the polarization angle. The polarization angle is chosen such a way that  $F_+$  is 1 and  $F_\times$  is 0. Finally the strain produced at the detector by the black hole ringdown is given by,

$$h(t) = A_{RD} \cos(-2\pi f_{QNR} (t - t_0) + \gamma_0) e^{\left(\frac{-(t-t_0)^2}{2\tau^2}\right)} \quad (10)$$

where  $\gamma_0$ , is the initial phase of the waveform. (For more details of the ringdown waveform see ref [7]).

### 3.5 Core collapse supernova waveforms

The supernova waveforms, since no analytical solution for the equations is achievable we used a simulated set of 54 rotational supernova core collapse models in axisymmetry<sup>[8]</sup> given in the GW catalogue in the Max Plank Institute for Astrophysics web page. These simulations are performed by authors, Dimmelmeier, Ott, Janka, Marek and Mueller, by solving the full general relativistic hydrodynamic equations, in a flux-conservative formulation<sup>[9]</sup> on a grid using spherical coordinates. In these simulations the strain in the detector is a dimensionless signal amplitude, at a distance of 10 kpc with optimal orientation of the source, i.e. measured in the equatorial plane. To allow the desired variation in the distance in the injections, the waves were rescaled back to the origin of 10 kpc and scaled to the desired distance.

## 4. Detection algorithm mHACR

In this section we give a brief description on mHACR. The algorithm was developed from HACR<sup>[3]</sup> which is an algorithm for the identification of short burst of gravitational radiation in the data from broadband interferometric detectors, such as GEO600. The algorithm starts by dividing the data  $h$ , in short segments and the discrete Fourier transform is computed after a suitable window function is applied.

The length of each segment is chosen from the duration of the expected signal (ranges from a few milliseconds to a few tens of milliseconds). Then it creates a spectrogram of the data segment to be analyzed<sup>[4]</sup>, which represents a two dimensional energy density function in the time of interest.

After constructing the spectrogram, time-frequency pixels which are statistically different from the background noise are identified. It first estimates the mean and standard deviation of each frequency bin of each row of the spectrogram. This is done by calculating the “significance” of each time-frequency pixel, each time-frequency pixel is assigned a color (black, gray and white) based on its significance and chosen upper and lower thresholds. Neighboring time-frequency pixels with high significance (with color black or grey) are clustered to form “burst events”, and then it proceeds to parameterize the event in terms of a few parameters (for further explanation see ref [4]).

## 5. Hardware injection of burst waveforms

The parameter ranges for the unphysical and burst waveforms, is chosen such that injected signals to span a sensible range of signal to noise ratio (SNR) at the detector

output (not too small to be undetected by mHACR and not too big to be unrealistic). Table 1 and table 2 shows the ranges used for the ad-hoc and physical waveforms, respectively.

*Table 1. Ranges of the parameters for the ad-hoc waveforms used in the series of the injections*

Parameter	Min	Max
$h_{rss}$	$5 \times 10^{-21}$	$5 \times 10^{-20}$
$\tau$ (s)	$3 \times 10^{-3}$	$1 \times 10^{-2}$
$f_o$ (Hz)	200	1200
$Q$	8.7	9.1
$t_o$ (s)	$t/4$	$3t/4$

*t, length of the time interval of each waveform,  $0 < t < 1-1/f_o$ , in seconds*

*Table 2. Ranges of the parameters for the physical waveforms used in the series of the injections*

Parameter	Min	Max
$M_{ringdown}$ ( $M_{\odot}$ )	10	100
$d_{supernova}$ (kPc)	.2	1
$d_{ringdown}$ (MPc)	200	2000

In the case of ring down waveform, it is assumed that  $\varepsilon = 1.5 \times 10^{-2}$ , fraction of the black hole mass radiated as GWs. Also we choose the initial phase  $\gamma_o$  to be  $\pi/2$  in order to avoid sharp edges in the ring down waveform. The coalescing binary is assumed to have equal masses, so that  $\eta = 0.25$ .

The hardware injections were done for 9 hours, making 756 injections. Which were injections by: 197 supernova core collapses, 194 sine-Gaussians, 173 blackhole ringdowns, 97 Gaussians distributions and 96 Gaussian noise bursts.

In the 9 hrs of injection time 1244 and 875 events were found in the  $h(t)$  and the injection channel respectively, with SNR greater than 10. Searching for coincidences in these two sets of events yielded 694 coincidences, In order to determine coincidences, we used a time-coincidence window of 5 ms and a frequency coincidence window of 1500 Hz.

Amplitude spectral density (ASD) of one sine-Gaussian waveform among the injected ones is shown in Fig. 2. The Trace on top shows (green line) the spectral density of the waveform measured in the injection channel, and the plot on the bottom shows the ASD of the  $h(t)$  data (red line) at the time of this injection. Also overlaid is the ASD of the injected waveform (blue line). It can be seen that, as expected, the sine-Gaussian has a symmetric spectrum centered around a well-defined central frequency. Because of the well-defined signal characteristics, mHACR is able to make a very good estimation of the parameters of the sine-Gaussian injections.

ASD of one example Gaussian waveform is plotted in Fig. 3. As in the previous figure, the trace on top shows (green line) the spectral density of the waveform measured in the injection channel, and the plot on the bottom shows the ASD of the  $h(t)$  data (red line) at the time of this injection. Also overlaid is the ASD of the injected waveform (blue line). It can be seen that, unlike the sine-Gaussians, the Gaussian waveforms don't have a well-defined central frequency. Moreover, since the spectrum is asymmetric the central frequency estimation is affected by the shape of the noise floor. We thus expect larger errors in the parameter estimation by mHACR for these waveforms. Gaussians-modulated noise bursts present more difficulties in its parameterization and their detection altogether.

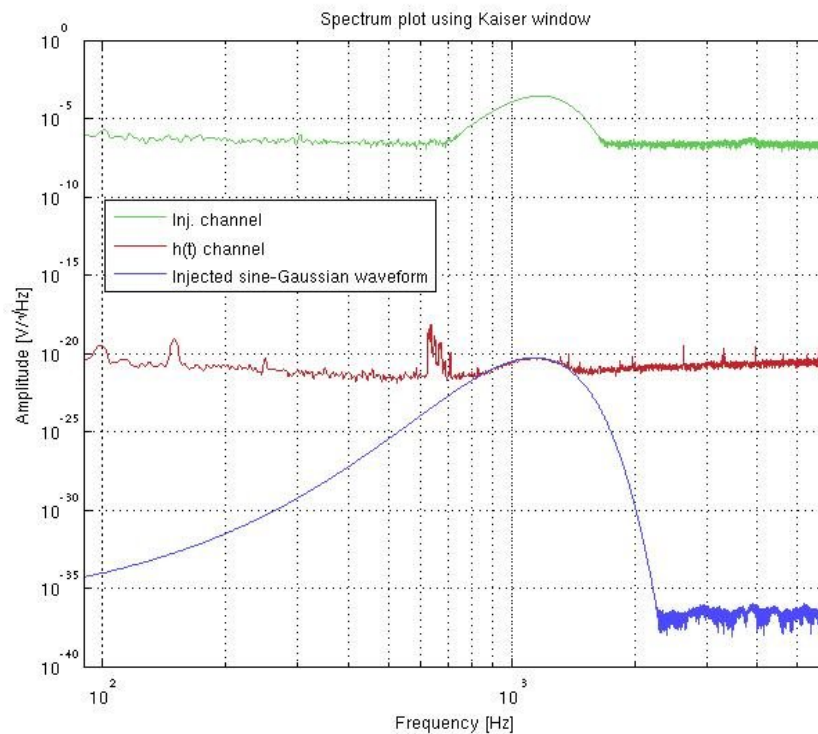


Figure 2. ASD of a simulated Sine-Gaussian (in blue), compared to the signal found in  $h(t)$  (red) and in the injection channel (green).

As the blue line in fig. 4 shows, the power in these waveforms will be distributed over a wide range of frequencies, that is because of the noise component. Its pseudorandomness properties will distribute the power (blue line) over the whole frequency spectrum, allowing this waveform to be much harder to detect as is seen from the red line, the spectrum of this injection fell below the GEO threshold (red line), so only very noisy Gaussian noise bursts will be detected, not a high expectancy of these should be expected. This is because the power spectrum of white noise, as the name indicates, is flat. Unless these waveforms are injected with very high ASDs, they lie below the noise floor of the detector, and are often undetectable by mHACR.

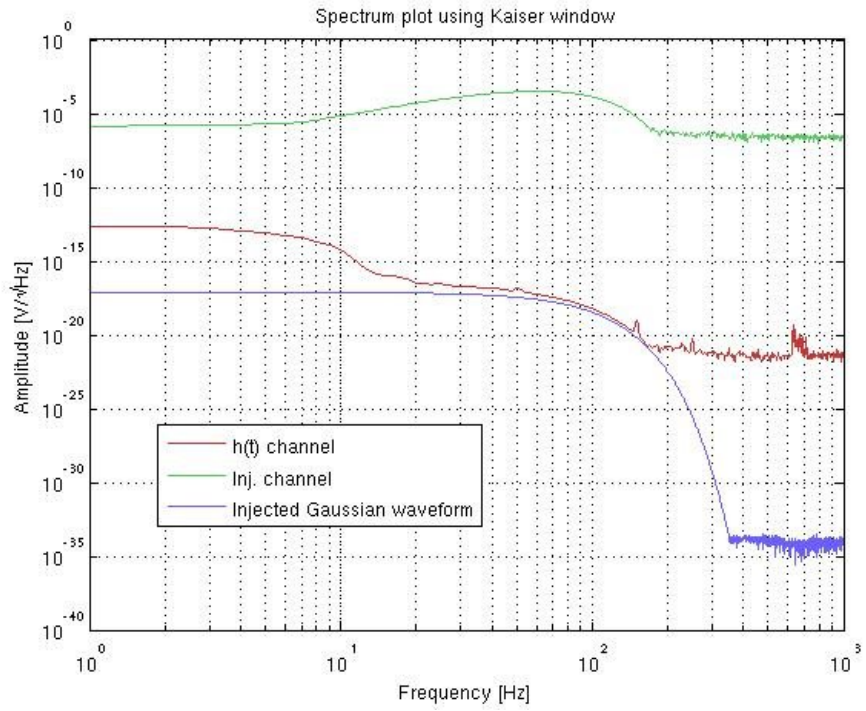


Figure 3. ASD of Gaussian distribution (in blue) compared with Gaussian found in  $h(t)$  (red) and in the injection channel (green)

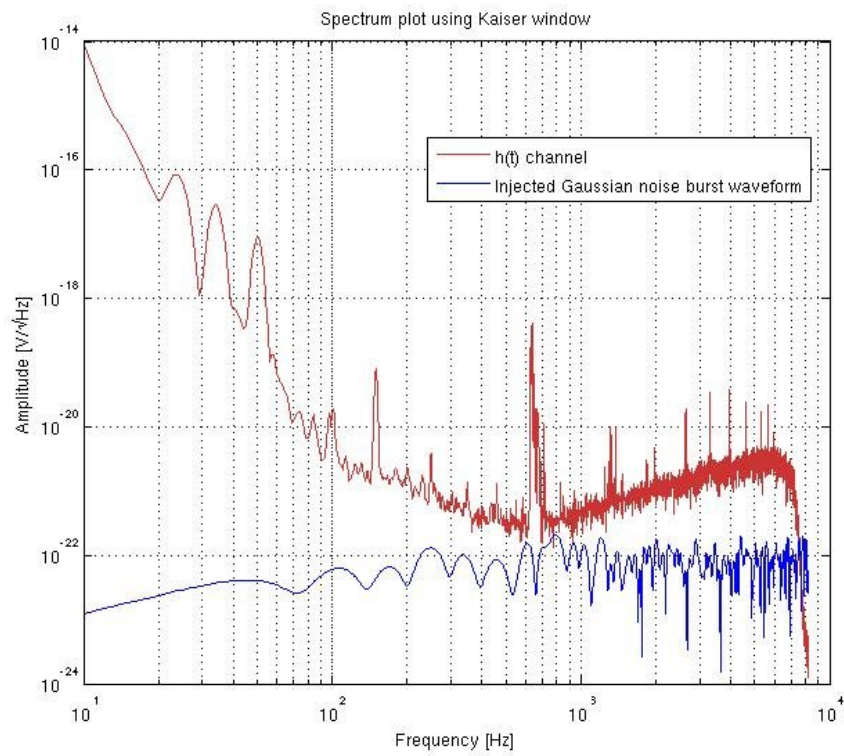


Figure 4. ASD of Gaussian Noise Burst (blue) compared to the sensitivity ASD of the strain in GEO (red).

Amplitude spectral density of a black hole ring down waveform is plotted in fig. 5. The spectrum of the ring down waveform is known to be a Lorentzian function with a well-defined characteristic frequency. We expect that mHACR estimates the parameters of these waveforms reasonably well, though, since the spectrum is asymmetric, we expect some bias in the estimated central frequency. Comparing the green line, the injected waveform, to the red line, the detected signal, it is easily seen that at higher frequencies the central frequency estimation will be shifted to lower frequencies. So for very loud and lower frequency events it should be properly estimated, since most of the power will be detected in the  $h(t)$ , and won't fall below the increasing GEO threshold. As the ringdown the same analysis is done for the supernova core collapse, at lower frequencies it will be readily detected and estimated meanwhile at higher frequency injections will be detected at lower frequencies.

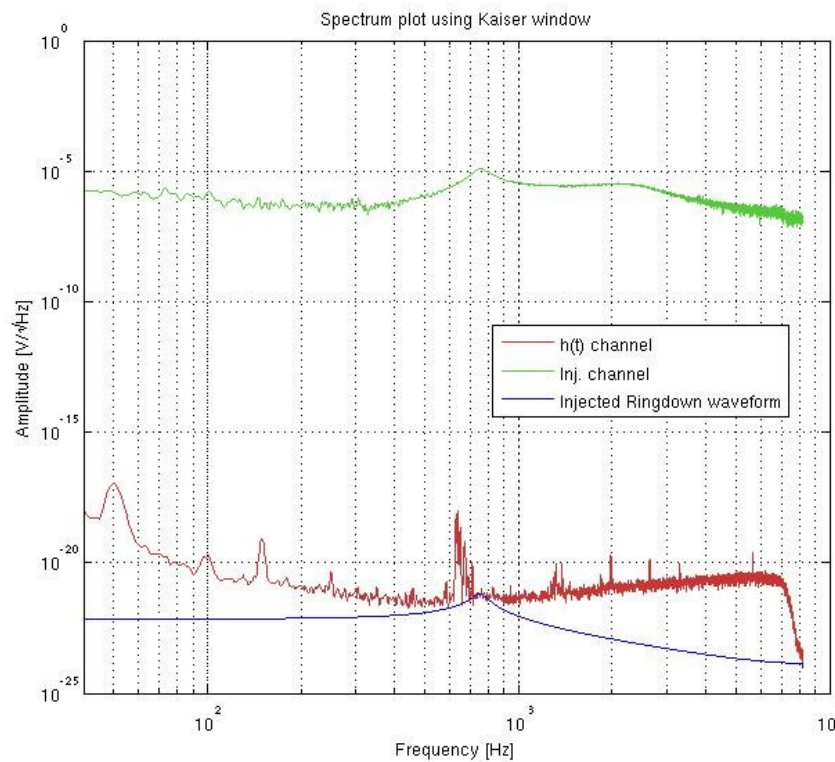


Figure 5. ASD of a simulated blackhole ringdown (blue) compared to the detected signal in  $h(t)$  (red) and in the injection channel (green)

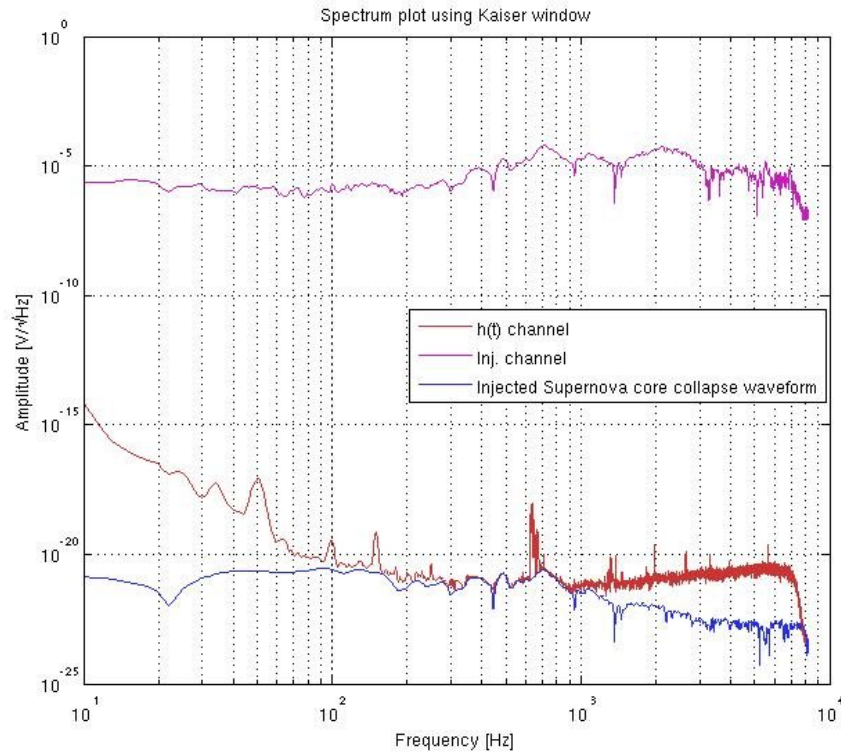


Figure 6. ASD of a simulated supernova core collapse (blue) compared with the signal in  $h(t)$  (red) and in the injection channel (purple)

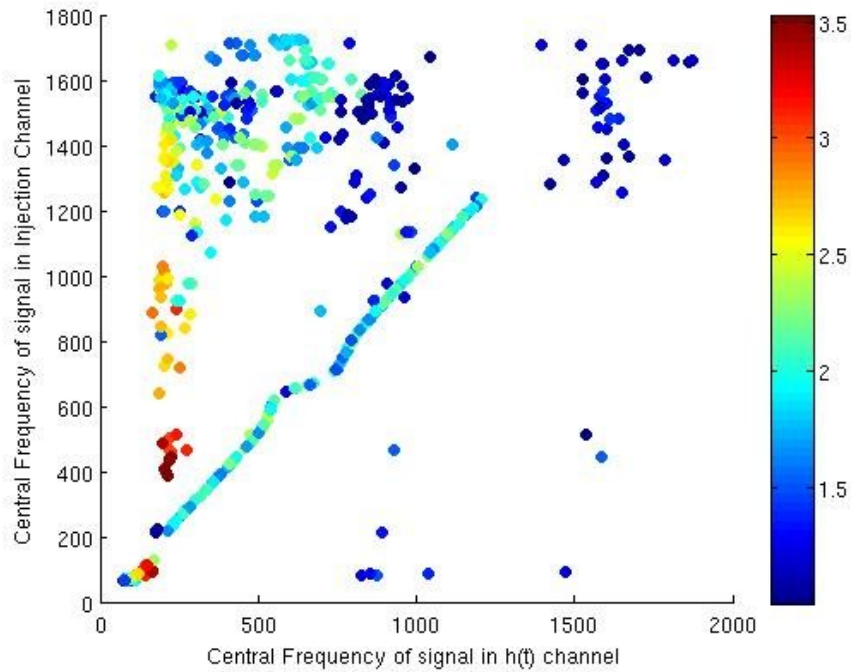


Figure 7. Graph of detected signal central frequency as a function of injected signal central frequency.

In Fig. 7, we plot the central frequency of the burst waveforms in the injection channel against the same in the  $h(t)$  channel, as estimated by mHACR. A straight line is clearly

seen in the center which corresponds, mostly, to sine-Gaussian waveforms<sup>†</sup>. Owing to the well-defined characteristics of these waveforms, quality of the central frequency estimation is adequate. Owing to the lack of well-defined signal characteristics and some other complexities in the parameter estimation, the central frequency estimation for many other waveforms is inadequate. While detailed studies are required in order to properly characterize the quality of parameter estimation of mHACR on these wide morphology of waveforms, this study may be viewed as a preliminary step in this direction

## Summary

In this report we presented an improved comprehensive injection pipeline for GEO600, it injects a wide variety of physical and ad-hoc waveforms. Preliminary test on the injection pipeline was successfully done by making hardware injection in GEO600. These injections were readily detected by mHACR by making time coincidence test on the injection channel and the detection channel. A display a straight line in the trace of injected against detected triggers, suggesting the sine-Gaussians injection and many dispersed signals owed to the complexity of parameter estimation as expected.

## Acknowledgements

I would like to thank Martin Hewitson and Pamareswaran Ajith for the help and guidance in these past two months. I would also like to thank the NSF, and the University of Florida for funding, also GEO-600 and the Universität Hannover for allowing me to use its facilities.

## References

- [1] B. Abbott, R. Abbott and R. Adhikari, & coll. Nucl.Instrum.Meth. A517 (2004) 154-179
- [2] M. Hewitson and P. Ajith. Class.Quant.Grav. 22 (2005) 4903-4912
- [3] J. Sylvestre. Phys. Rev. D 66 102004 (2002) 66-89
- [4] S. Hild, P. Ajith, M. Hewitson, H Grote and J.R. Smith. Class.Quant.Grav. 24 (2007) 3783-3798
- [5] S. Heng, R. Balasubramanian, B.S. Sathyaprakash and F.B. Schutz Class.Quant.Grav. 21 (2004) S821-S826
- [6] R. Balasubramanian, H. Grote, I.S. Heng, M. Hewitson, H. Lück, J. R. Smith, K. A. Strain, H. Ward and B. Willke. Class.Quant.Grav. 22 (2005) 3015-3028
- [7] M. Luna and A. Sintes. Class.Quant.Grav. 23 (2006) 3763-3782
- [8] H. Dimmelmeier, C. D. Ott, H.T. Janka, A. Marek and E. Mueller. arXiv:astro-ph/0702305v2
- [9] F. Banyuls, J. Font, J. Ibañez, J. Marti and J. Miralles. The Astrop. Journ. 476 (1997) 221-231

---

<sup>†</sup> The wavy line in the middle of fig. 7 is due to a filter in GEO to eliminate the violin modes of the main suspension fibres in GEOs environment around the 700 Hz. It can be seen in all of the red lines of figures 2-6.